Astron. Astrophys. 353, 108–116 (2000)

ASTRONOMY AND ASTROPHYSICS

The role of Kelvin-Helmholtz modes in superwinds of primeval galaxies for the magnetization of the intergalactic medium

G.T. Birk[1], **H. Wiechen**[1], **H. Lesch**[1], **and P.P. Kronberg**[2]

[1] Institut für Astronomie und Astrophysik der Universität München, Scheinerstrasse 1, 81679 München, Germany
[2] Department of Physics, University of Toronto, 60 St George, Toronto, M5S 1A7, Canada

Received 30 July 1999 / Accepted 26 October 1999

Abstract. Superwinds of primeval dwarf galaxies seem to play an important role in the early magnetization of the intergalactic medium. Realistic estimates of the "ultimate", post-outflow diffuse intergalactic magnetic field strengths cannot be made with simple flux conservation arguments. Rather one has to consider dynamical field regeneration mechanisms. Furthermore the role of the neutral component of the superwind outflow gas needs to be taken into account since local-universe outflow winds are known to be only partially ionized.

Kelvin-Helmholtz instabilities are one plausible candidate for the amplification of magnetic flux expelled from the starbursting primeval galaxies. We examine solutions of the analytically derived generalized dispersion relation that is valid for partially ionized plasmas. Our calculations indicate that Kelvin-Helmholtz modes can operate fast enough to amplify the magnetic field strengths in superwinds within the timescale of the outflow.

Plasma-neutral gas simulations show that the non-linear evolution of the Kelvin-Helmholtz modes resemble the pure MHD one and corroborate the idea that the coupling of the neutral and ionized components is sufficient to convert the free energy supplied by the superwinds to magnetic field energy.

We argue that further amplification can be expected due to the development of smaller vortices and sharper magnetic field gradients during the continuous injection of magnetic flux.

Key words: galaxies: magnetic fields – galaxies: intergalactic medium – galaxies: dwarf – galaxies: starburst – instabilities – plasmas

1. Introduction

Hierarchical models of structure formation suggest that dwarf galaxies are the building blocks of larger galaxies, merging at high redshifts to form the today's distribution of galaxies (e.g. Padmanabhan 1993 and references therein; Tegmark et al. 1997). It is therefore crucial to understand both their formation and evolution. Besides the importance for the formation of spiral and elliptical galaxies, dwarf galaxies are ideal targets for investigation of the interrelations between galaxies and the contents and dynamics of the intergalactic medium, since dwarfs are known to support strong outflows via efficient and fast starburst events with accompanying supernova activity (cf. Heckman 1998 and references therein). The fact that the bolometric infrared luminosity, an indicator of starforming intensity, shows little correlation with galaxy rotation speed (an indicator of galaxy mass) over 5%- 100% of M(L_*), suggests that early generations of premerged starbursting dwarfs had vigorous outflow phases, aided by their low escape velocities (cf. MacLow & Ferrara 1999).

The intergalactic medium is enriched with metals (e.g. Renzini 1997); it also contains large-scale magnetic fields, at least in and around clusters of galaxies (cf. Kronberg 1994). The metallicity enhancement of the intergalactic medium can be explained by galactic winds from starbursting dwarfs (Trentham 1994; Nath & Chiba 1995). Kronberg et al. (1999) have shown that the observed magnetization of the intergalactic medium (IGM), in principle, can also be caused by primeval starbursting dwarf galaxies. They used model calculations and present-day starburst galaxies to show that a significant fraction of the intergalactic medium can be filled with magnetic fields that originally emanated from the transport of magnetic flux into the IGM from primeval dwarf galaxies. Evidence for strong, magnetized outflows come from observations of M82 (e.g. Reuter et al. 1992; Shopbell & Bland-Hawthorn 1998), NGC 3079 (e.g. Duric et al. 1983), NGC 4631 (e.g. Hummel et al. 1988) and NGC 4666 (e.g. Dahlem et al. 1997), all of which have superwinds and bubbles as magnetohydrodynamical consequences of the mechanical energy deposited inside starbursts (cf. also Heckman 1998 and references therein).

The calculations of Kronberg et al. (1999) focused on the volume distribution in the IGM of magnetic flux, and did not attempt a quantitative prediction of its strength. Recently, Birk et al. (1999) have shown that in the rather complex filamentary outflow of M82 (cf. Reuter et al. 1992; McKeith et al. 1995) unstable Kelvin-Helmholtz (KH) modes can be excited and that these result in magnetic field regeneration. They concluded that these KH modes can be responsible for the relatively strong and ordered halo magnetic fields. The resulting fields show significant deviation from estimates based on flux conservation only. The amplification of magnetic fields in magnetized plasma flows

Send offprint requests to: G.T. Birk (birk@usm.uni-muenchen.de)

due to a strong curling and twisting of field lines in magnetized boundary layers is a generic feature of KH modes (e.g. Clarke 1993; Frank et al. 1996).

In this contribution we focus on the role of KH instabilities in superwinds of primeval galaxies. We consider a situation which is characterized by the interaction of the galactic winds and the IGM. Whereas one should expect a huge number of KH resonant layers that are convected by the outflowing material and may interact with each other, as a first step, we will concentrate on one KH unstable boundary layer.

The winds and the IGM may be *partially ionized*, in particular, at very early epochs of the newly formed dwarf galaxies at which neutral gas is a large component of the galaxy's mass. Moreover, some of the expelled hot wind plasma cools and may fall back (probably into a neighbouring galaxy) as a mixture of ionized and neutral gas, thereby interacting with outflowing plasma in the process. This type of scenario is supported by observations of present day superwinds, that clearly indicate that neutral gas is a significant component of the material expelled from the galactic plane of starburst galaxies (e.g. Heckman et al. 1993; Weiß et al. 1999).

The consequence of this is that a two-fluid treatment of KH dynamics rather than a pure MHD description seems to be the appropriate approach to understanding the evolution of the field, and the energy equipartition. For recent detailed investigations of KH modes in the pure MHD regime see Frank et al. (1996) and Miniati et al. (1999) and references therein. In the next section we develop analytic estimates of the relevant time scales of the KH modes. These estimates are based on the analysis of the general dispersion relation of unstable KH modes in *partially ionized* plasmas. They take account of the different bulk velocities and mass densities of both the neutral and the ionized gas components on both sides of the KH interface. In Sect. 3 we present numerical simulations that model the KH dynamics in a self-consistent way.

2. Kelvin-Helmholtz instabilities in superwinds of primeval galaxies: analytical estimates

The dynamics of partially ionized dissipation-free two-fluid plasmas in ionization equilibrium is determined by balance equations describing the conservation of mass and momentum of both plasma and neutral gas

$$\frac{\partial \rho}{\partial t} = -\nabla \cdot (\mathbf{v}\rho) \tag{1}$$

$$\frac{\partial \rho_n}{\partial t} = -\nabla \cdot (\mathbf{v_n}\rho_n) \tag{2}$$

$$\frac{\partial}{\partial t}(\rho \mathbf{v}) = -\nabla\cdot(\rho \mathbf{v}\mathbf{v}) - \nabla p + \frac{1}{4\pi}(\nabla \times \mathbf{B}) \times \mathbf{B} - \rho\nu(\mathbf{v}-\mathbf{v_n}) \tag{3}$$

$$\frac{\partial}{\partial t}(\rho_n \mathbf{v_n}) = -\nabla \cdot (\rho_n \mathbf{v_n}\mathbf{v_n}) - \nabla p_n + \rho\nu(\mathbf{v} - \mathbf{v_n}) \tag{4}$$

and the induction equation that governs the temporal evolution of the magnetic field

$$\frac{\partial \mathbf{B}}{\partial t} = \nabla \times (\mathbf{v} \times \mathbf{B}). \tag{5}$$

In these equations ρ, $\mathbf{v}$, p, $\mathbf{B}$ and c denote the plasma mass density, velocity, thermal pressure, the magnetic field and the velocity of light. The lower index n identifies neutral gas quantities. The final terms in Eqs. (3) and (4) specify the rate of momentum transfer between the ionized and the neutral gas components. This is proportional to the effective plasma-neutral gas collision frequency ν. For the analytical calculation of the dispersion relation for KH modes we assume incompressibility.

In the subsequent numerical simulations described in Sect. 3 we will remove the restriction of incompressibility.

The KH dispersion relation can be obtained by standard linear mode analysis. Ershkovich and co-workers have extensively analyzed KH modes, with applications to partially ionized cometary ionopauses. Ershkovich and Mendis made use of a one-fluid description which holds for the strong coupling régime only (Ershkovich & Mendis 1983). A multi-fluid approach allows for an explicit treatment of collisional momentum transfer which has been investigated for both compressible (Ershkovich & Mendis 1986), and incompressible cases (Ershkovich et al. 1986a, b). Neither of the two contributions cited above takes into account the thermal pressure forces of the neutral component, or perturbations in the neutral gas bulk velocities. This is justified for the application to cometary ionopauses but not for the application to multi-phase galactic outflow winds. Also we do not restrict ourselves to uniform media with negligible thermal neutral gas pressure, as was done by Bhatia and Steiner (1974).

In this paper we take into account the full incompressible dynamics of both the neutral and the ionized gas components. Doing this we find the following dispersion relation for KH modes (for details of the corresponding analysis see Appendix):

$$\begin{aligned}
&16\pi^2 i(\nu\overline{\tilde{\omega}_n\rho^{eq}} - \overline{\tilde{\omega}_n^2\rho_n^{eq}})^2\overline{\tilde{\omega}^2\rho^{eq}}^2 \\
&+8\pi[B^{eq^2}k_z^2(-i\nu^2\overline{\tilde{\omega}_n\rho^{eq}}^2 + i\overline{\tilde{\omega}_n^2\rho_n^{eq}}^2 - 2\nu\overline{\tilde{\omega}_n\rho^{eq}}\,\overline{\tilde{\omega}_n^2\rho_n^{eq}}) \\
&+4\pi\nu\overline{\tilde{\omega}\rho^{eq}}(\overline{\tilde{\omega}_n^2\rho_n^{eq}}^2 + i\nu\overline{\tilde{\omega}_n\rho^{eq}}\,\overline{\tilde{\omega}_n^2\rho_n^{eq}})]\overline{\tilde{\omega}^2\rho^{eq}} \\
&+B^{eq^4}k_z^4(-i\overline{\tilde{\omega}_n^2\rho_n^{eq}}^2 + 2\nu\overline{\tilde{\omega}_n\rho^{eq}}\,\overline{\tilde{\omega}_n^2\rho_n^{eq}} + i\nu^2\overline{\tilde{\omega}_n\rho^{eq}}^2) \\
&-8\pi B^{eq^2}k_z^2\nu\overline{\tilde{\omega}\rho^{eq}}\,\overline{\tilde{\omega}_n^2\rho_n^{eq}}(i\nu\overline{\tilde{\omega}_n\rho^{eq}} + \overline{\tilde{\omega}_n^2\rho_n^{eq}}) \\
&+16\pi^2 i\nu^2\overline{\tilde{\omega}\rho^{eq}}^2\overline{\tilde{\omega}_n^2\rho_n^{eq}}^2 = 0
\end{aligned} \tag{6}$$

where the superscript eq denotes equilibrium values and k_z is the wave number parallel to the KH interface. The bar indicates mean values across the KH interface. The Doppler shifted complex growth rate is denoted by $\tilde{\omega} = \omega - k_z v^{eq}$ or $\tilde{\omega}_n = \omega - k_z v_n^{eq}$, respectively.

For one-fluid MHD systems the stability criterion for KH modes can be stated as follows (e.g. Woods 1987)

$$(\mathbf{k}\cdot\mathbf{v}_{rel})^2 \geq \frac{\rho_I + \rho_{II}}{4\pi\rho_I\rho_{II}}[(\mathbf{k}\cdot\mathbf{B}_I)^2 + (\mathbf{k}\cdot\mathbf{B}_{II})^2] \tag{7}$$

where $\mathbf{B}_I$ and $\mathbf{B}_{II}$ denote the magnetic field on both sides of the boundary layer, and ρ_I, ρ_{II} denote the corresponding mass densities. (Note that I and II here do not refer to the neutral and ionized components.) However, in the case of interacting flows of ionized and neutral gas components this onset criterion is no longer required to be fulfilled for KH modes to be excited.

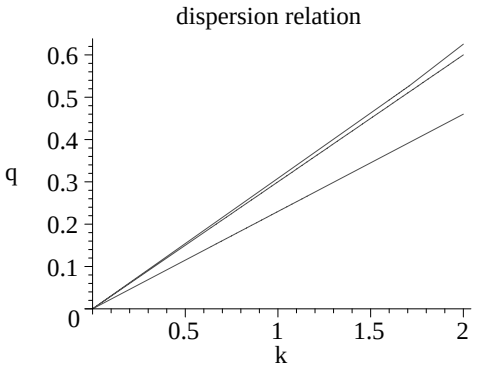

Fig. 1. a Dispersion relation of the KH modes in a partially ionized regime. The normalized growth rate q is plotted against the normalized wave number k. The solutions are obtained for the normalized parameter sets (from top to bottom): $B = 10^{-6}$, $v_I = 0.8$, $v_{nI} = 0.6$, $v_{II} = v_{nII} = 0$, $\rho_I = \rho_{II} = 0.1$, $\rho_{nI} = \rho_{nII} = 1.0$, $\nu = 10^5$; $B = 10^{-6}$, $v_I = v_{nI} = 0.6$, $v_{II} = v_{nII} = 0$, $\rho_I = \rho_{II} = 0.1$, $\rho_{nI} = \rho_{nII} = 1.0$, $\nu = 10^5$ and $B = 10^{-5}$, $v_I = v_{nI} = 0.8$, $v_{II} = v_{nII} = 0$, $\rho_I = \rho_{nI} = 1$, $\rho_{II} = \rho_{nII} = 0.1$, $\nu = 10^5$. The normalizing quantities are $B_0 = 10^{-4}$G, $v_0 = 10^8 \mathrm{cms}^{-1}$, $\rho_0 = 0.1 m_p$ and $L_0 = 1$kpc. Thus, a normalized growth rate of $q = 1$ means a linear growth time of the KH mode of $t_{KH} = 10^{13}\mathrm{s} = 3.2 \cdot 10^5$yr. For the solutions **b** (different bulk velocities v and v_n) and **c** (equal bulk velocities v and v_n) the pure MHD criterion Eq. (7) is not fulfilled.

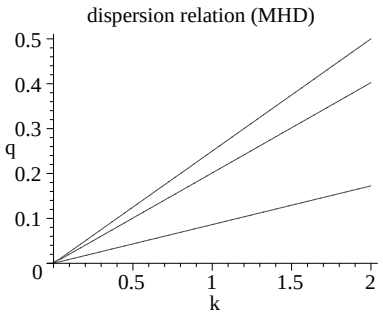

Fig. 2. Dispersion relation for the pure MHD KH modes for the normalized parameter sets (from top to bottom): $B = 10^{-6}$, $v_I = 0.7$, $v_{II} = 0.2$, $\rho_I = \rho_{II} = 1.0$; $B = 10^{-6}$, $v_I = 0.7$, $v_{II} = 0$, $\rho_I = 1.0$, $\rho_{II} = 0.1$, and $B = 10^{-5}$, $v_I = 0.3$, $v_{II} = 0$, $\rho_I = 10.0$, $\rho_{II} = 1.0$. The normalizing quantities are the same as in Fig. 1.

To exemplify this, Fig. 1 shows dimensionless solutions of the dispersion relation for different choices of the normalized mass densities, velocities, magnetic field strengths, and effective collision frequencies. The real part of the normalized growth rate q, which is the inverse normalized growth time, is plotted against the normalized wave number $k = 2\pi/\lambda$ (where λ is the dimensionless wave length). As in the one-fluid case we find non-dispersive modes which are, however, overstable ones (at this point we are not interested in the oscillatory part of the complex growth rates).

From the results shown in Fig. 1 we can get quantitative estimates of the linear time scales of the KH modes by normalizing to physical parameters that are typical of galactic superwinds. We have chosen the following typical plasma values (indicated by the index 0); $\rho_0 = 0.1 m_p \mathrm{cm}^{-3}$ (m_p being the proton mass), and wind velocity $v_0 = 10^8 \mathrm{cms}^{-1}$. Since the velocities are formally normalized to the Alfvén speed $v_A = B_0/(4\pi\rho_0)^{1/2}$ the choice of $v_0 = v_A$ implies $B_0 = 10^{-4}$G. This choice is motivated by observational data from the prototypical starburst galaxy M82 (e.g. Lehnert & Heckman 1986; Shopbell & Bland-Hawthorn 1998). One may speculate on the appropriate neutral gas density. Here, we have in mind a situation where neutral gas is still falling onto the central region of a young primeval dwarf galaxy and/or one in which the outflow wind has a significant neutral/molecular gas component. As a typical magnetic field strength we choose $B = 10^{-6} B_0 = 10^{-10}$G (and for comparison $B = 10^{-5} B_0$) which can be expected from the compressional amplification of some seed fields during the collapse dynamics (cf. Lesch & Chiba 1995). For the wavelength we choose, for example, the typical extension of observed radio filaments in M82, i.e. $\lambda_0 = 1$ kpc (Reuter et al. 1992).

The typical time scales of the KH instability can now be calculated from the inverse growth rate (see Fig. 1) $t_{KH} = q^{-1}\lambda_0/v_0 = 3.2 \cdot 10^5 q^{-1}$yr. This means that even for relatively large characteristic length scales of 1kpc the KH dynamics has enough time for the regeneration of the magnetic fields that are transported by the superwinds given expected lifetimes of the bursts of some 10^7 yr (cf. Rieke et al. 1980; Mateo 1998). For different choices of the normalizing quantities, the inherent time scales for the linear dynamics of the KH modes can accordingly be found from Fig. 1. It should be noted that the choice of $\lambda_0 = 1$kpc results in quite a high limit for the linear growth time of the KH modes since one should expect the KH instability to operate in thinner boundary layers.

For comparison Fig. 2 shows solutions of the KH dispersion relation for the pure MHD case. It can be seen that comparable flow conditions in the MHD, and the partially ionized régime result in quite similar growth times of the unstable modes. This means that KH modes are expected to amplify the magnetic field as efficiently as in the totally ionized MHD régime. This result is important, given the considerable uncertainties, and likely variations in the physical parameters that characterize the interaction details of superwinds and infall gas in primeval galaxies.

What we can conclude is that magnetic field amplification by KH modes can occur effectively during the entire life time of the primeval dwarf galaxies or the starbursts, respectively (cf. Mateo 1998), and that it is relatively insensitive to varying degrees of ionization in the interacting gas flows. What cannot be derived from the linear analysis is the amplification factor. However it can be obtained by nonlinear simulations, which we present in following section.

3. Kelvin-Helmholtz instabilities in superwinds of primeval galaxies: simulation results

Whereas in the preceding section we described an analytic treatment of the linear evolution of the KH mode in partially ionized plasmas, in this section we show results of numerical simulations of the linear and non-linear evolution of KH modes in the appropriate parameter régime. These first self-consistent simu-

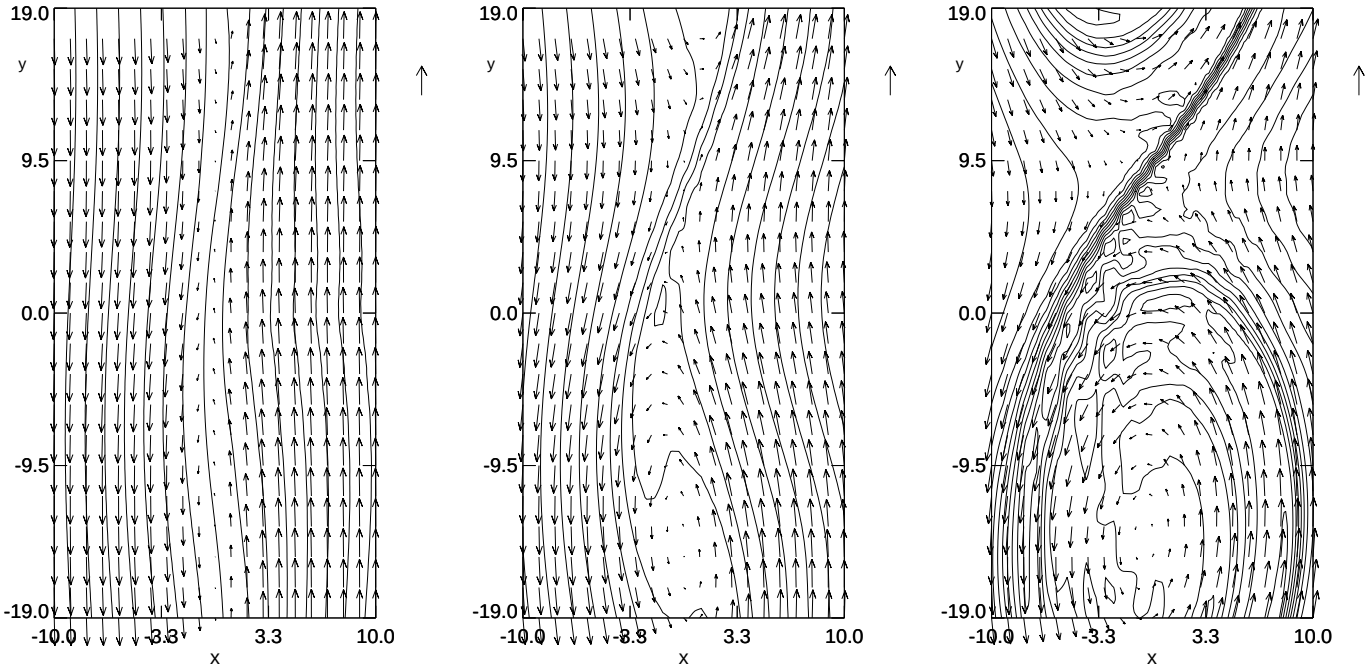

Fig. 3. Ionized gas flow (indicated by arrows) in the x-y-plane. The solid lines indicate the magnetic field. Snapshots of the evolution of the KH mode are shown at $t = 50t_A$ (left plot), $t = 100t_A$ (middle plot) and $t = 200t_A$ (right plot). The lengths of the exposed arrows indicate flow velocities of 1.08, 1.20 and 1.28 times the initial amplitude.

lations of the full KH dynamics in 2-fluid systems are carried out with an explicit plasma-neutral gas fluid code (Birk & Otto 1996). As distinct from analytical estimates for the linear evolution of the KH modes we do not need to assume incompressibility, and we now include the balance equations for the thermal pressures of both the ionized and the neutral gas components (p and p_n). These equations are

$$\frac{\partial p}{\partial t} = -\mathbf{v}\cdot\nabla p - \gamma p \nabla\cdot\mathbf{v} - (\gamma-1)\nu\left(\left(p-\frac{\rho}{\rho_n}p_n\right) - \rho\left(\mathbf{v}-\mathbf{v}_n\right)^2\right) \quad (8)$$

$$\frac{\partial p_n}{\partial t} = -\mathbf{v}_n\cdot\nabla p_n - \gamma p_n\nabla\cdot\mathbf{v}_n + (\gamma-1)\nu\left(p-\frac{\rho}{\rho_n}p_n\right) \quad (9)$$

where we assume the same adiabatic index γ for both fluid components. The integration scheme is based on the Leapfrog algorithm that is of second order in space and time and has the advantage of very low numerical diffusion. Spurious magnetic reconnection due to uncontrolled numerical diffusion can be avoided almost completely (cf. discussion by Frank et al. 1996 and Birk et al. 1999). The balance equations are integrated in a dimensionless form. They are normalized by a typical magnetic field strength B_0, a typical mass density ρ_0, a characteristic length scale L_0, the Alfvén velocity $v_A = B_0/(4\pi\rho_0)^{1/2}$, the Alfvénic transit time $t_A = L_0/v_A$ and the magnetic pressure $p_0 = B_0^2/4\pi$. As in Sect. 3 we choose $\rho_0 = 0.1m_p$ and $L_0 = 1$kpc. The wind velocity is, as before, $v_0 = 10^8\mathrm{cms}^{-1}$ and the initial homogeneous magnetic field is chosen as $B = 10^{-6}B_0 = 10^{-10}$G. This order of magnitude can be expected from the compressional amplification of seed fields during the protogalactic collapse (cf. Lesch & Chiba 1995). It should be noted that alternative simulation runs with a somewhat stronger initial magnetic field do not differ significantly from the results shown and discussed below as long as Kelvin-Helmholtz modes can be excited. In particular, the magnetic field amplification is comparable and happens on almost the same timescale. This is to be expected since the energy density of the initial magnetic field is much smaller than the kinetic energy of the wind plasma.

In the present simulations we choose a small homogeneous background resistivity in order to smooth gradients that otherwise could give rise to numerical instabilities. For the effective collision frequency we choose $\nu = 10$. The constant background resistivity chosen corresponds to a magnetic Reynolds number of $S = 1000$. The effects of varying resistivity have been discussed by Birk et al. (1999). A lower background resistivity results in a slightly higher maximum magnetic field strength. The calculations are performed in a mean velocity observer frame. The wind proceeds in the y-direction (perpendicular to the galactic disk) and the wind fragment has a velocity gradient that is directed along the x-axes (parallel to the disk). We assume a shear flow corresponding to $\mathbf{v} = \mathbf{v}_n = \hat{v}\tanh(x)\mathbf{e}_y$ with an amplitude $\hat{v} = 0.55v_0$ for both the plasma and the neutral gas andthat both the plasma and the neutral gas are homogeneous, with an ionization rate of 1% ($\rho = 1$; $\rho_n = 100$).

For the simulations we use a 3-dimensional code with a start configuration mentioned above. However, here, we only resolve the 2-dimensional dynamics. The simulation box is given by $-25 \le x \le 50$, $-25 \le y \le 20$, and $-1 \le z \le 1$ in units of 1kpc. The numerical grid points are equidistant, and are chosen to be $203 \times 103 \times 5$. This means that we are not applying strict

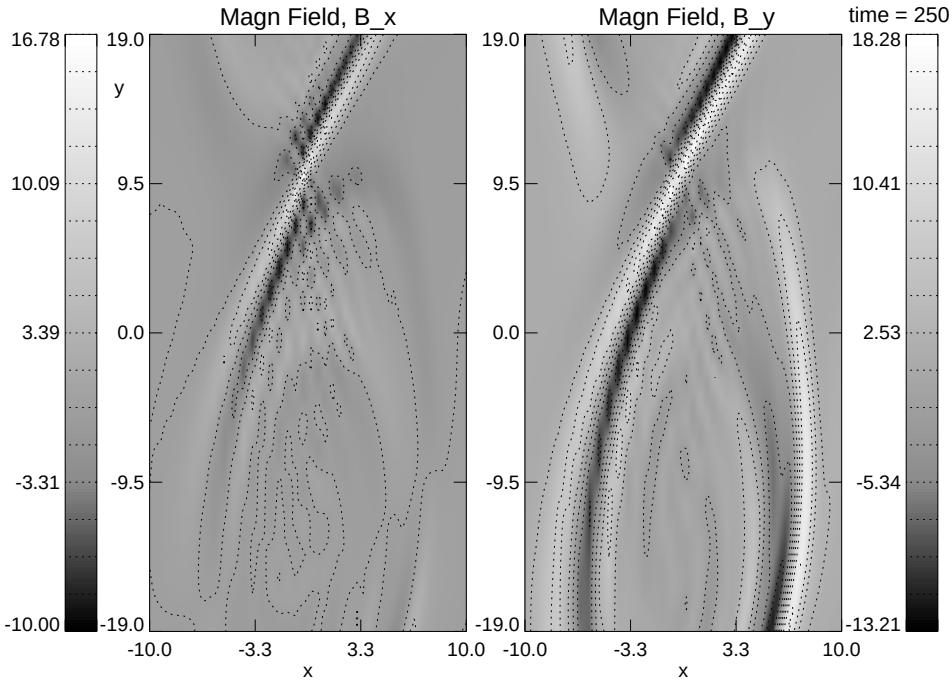

Fig. 4. The x- and y-component of the magnetic field after $t = 250t_A$. The amplitudes follow the KH vortex structure of the flow.

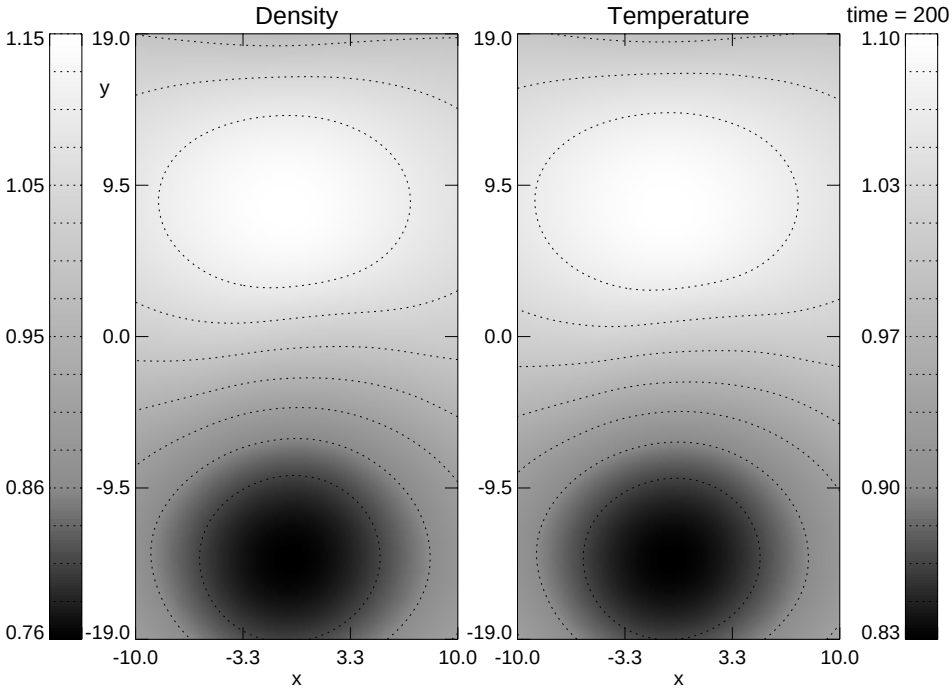

Fig. 5. Density and temperature of the ionized gas component after $t = 200t_A$. The compressible KH dynamics result in regions of depletion and cooling and compressional heating.

invariance in the third dimension but do not resolve the dynamics in the z-direction.

Fig. 3 illustrates the self-consistent evolution of the unstable KH mode after 50 (left plot), 100 (middle plot) and 200 (right plot) dynamical (Alfvénic transit) times, i.e. after 16Myr and 32Myr and 80Myr, respectively. Here, and in the following plots we show cuts at the $z = 0$-half plane. The arrows indicate the flow in the x-y-plane. Magnetic field lines are indicated by the solid lines The magnetic field lines become bent and the flow pattern develops the characteristic KH vortex structure after 100 dynamical times. After 250 dynamical times the KH mode has developed non-linearly. The magnetic field in the x-y-plane at this time is shown in Fig. 4. The curly structure can easily be identified. In the vicinity of the KH boundary layer magnetic field gradients steepen, and the field strength is intensified by a factor of about 20 after 200 Alfvénic transit times for the example shown. One recognizes that field amplification is not restricted to the boundary layer but is associated with the KH vortices (cf. also Fig. 6). We note that for a lower background resistivity sharper gradients form and the field line twisting increases. The z-component of the magnetic field remains zero for the chosen two-dimensional shear flow. The dynamics of

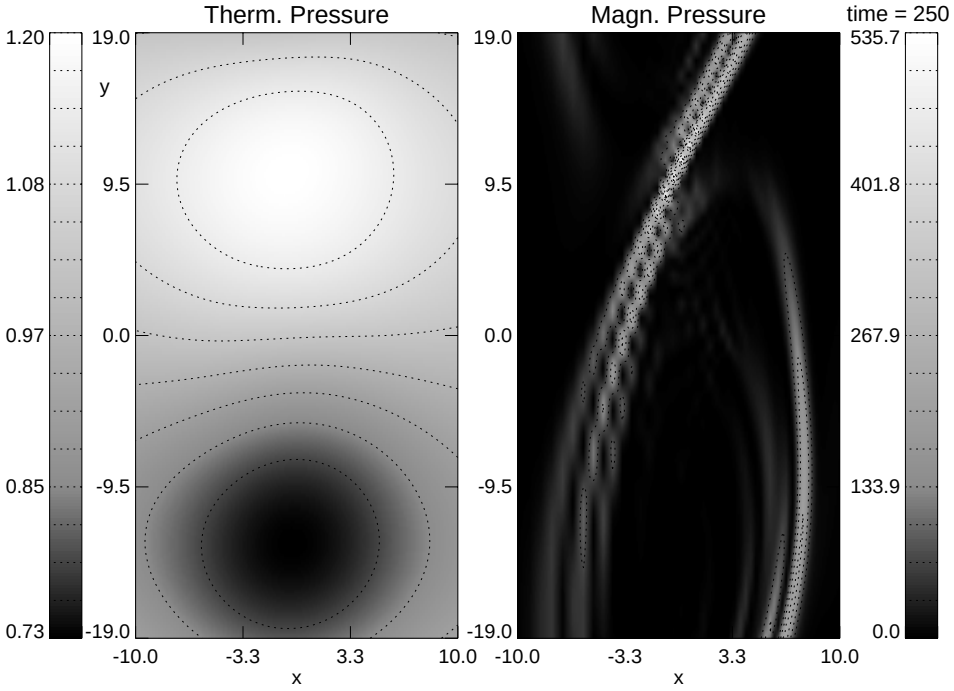

Fig. 6. Thermal pressure of the ionized gas and magnetic pressure after $t = 250t_A$.

the mode, in fact, is compressible (Fig. 5). The kinetic energy of the shear flow is mainly converted into magnetic energy rather than compressional heating (Fig. 6). The neutral gas component also shows the typical KH flow pattern (Fig. 7) with amplitudes enhanced by some 20% as it is the case for the ionized fluid component. As for the ionized component no significant flow in the z-direction occurs. The neutral gas density, as the mass density of the ionized component, show depletion and compression according to the evolution of the KH mode. Some fraction of the kinetic energy of the KH mode is converted into compressional heating (Fig. 8).

4. Discussion

It seems very likely that dwarf galaxies were the most abundant early structures in the Universe, and that they constituted "building blocks" for the formation of large present day galaxies. Superwinds of these primeval starbursting galaxies contribute efficiently to the magnetization of the IGM. In this contribution we have shown that unstable KH modes result in the rapid regeneration of the magnetic fields that are expelled, and thus, *can produce relatively strong field strengths in the immediately surrounding IGM* during this early epoch of galaxy formation. In our analysis we treated one single instability process excited by a linear mode perturbation. However, steady stellar activity in the dwarf galaxies should drive continuous winds that have KH unstable boundary layers. This will result in a continuous injection of amplified magnetic flux into the surrounding IGM. In our simulation study we find an amplification factor of about 20 for the parameters chosen. However, our quantitative result can only be regarded as an example for the parameters given and the only 2-dimensionally resolved dynamics. In really 3-dimensional configurations the evolution of the modes may be somewhat different (cf. Jones et al. 1999 for the pure MHD case). It can be expected that additional twisting in the third dimension allows for even stronger magnetic field amplification. More extensive numerical studies (see also below) are desirable and planned.

One may argue further that KH dynamics could produce even stronger magnetic field amplification. The development of KH vortices, and the consequent twisting and curling of magnetic field lines occurs on progressively smaller spatial scales as a turbulent cascade. Simple flux conservation arguments (cf. Biermann & Schlüter 1951) can be adduced to show that this process will continue until the local magnetic field is given by $B \leq B_{\rm max} = \sqrt{4\pi\rho}v_{\rm turb} = v_{\rm wind}(L_{\rm turb}/\lambda_0)^{1/3}$ ($v_{\rm turb}$, $L_{\rm turb}$ and $v_{\rm wind}$ are, respectively, the turbulent velocity, spatial dimension of the turbulence elements, and the macroscopic fluid velocity). For simplicity we have assumed Kolmogorov-type turbulence. Our choice of parameters leads to $B_{max} \approx 10^{-4}(L_{turb}/\lambda_0)^{1/3}$G. The magnitude of the amplification factor obtained by the KH simulations, $a_{KH} \approx 20$, suggests that further local turbulent magnetic field amplification can be effective down to spatial scales of $L_{turb} = (a_{KH}B_{in}/B_{max})^3\lambda_0 \approx 10^7$cm (where B_{in} is the initial magnetic field transported by the wind before the onset of the KH instability). Eventually, on very small spatial scales, redistribution by magnetic reconnection will become important. In this context a careful consideration of the electrical resistivity is necessary. It should be treated as a function of the current density, i.e. as a localized anomalous resistivity, rather than as a constant background value as chosen in our present study. The choice of the magnitude of such a resistivity is motivated by the relevant kind of violation of ideal Ohm's law, e.g. particle inertia or microturbulence, and will limit the amplification of the magnetic field as a real physical effect.

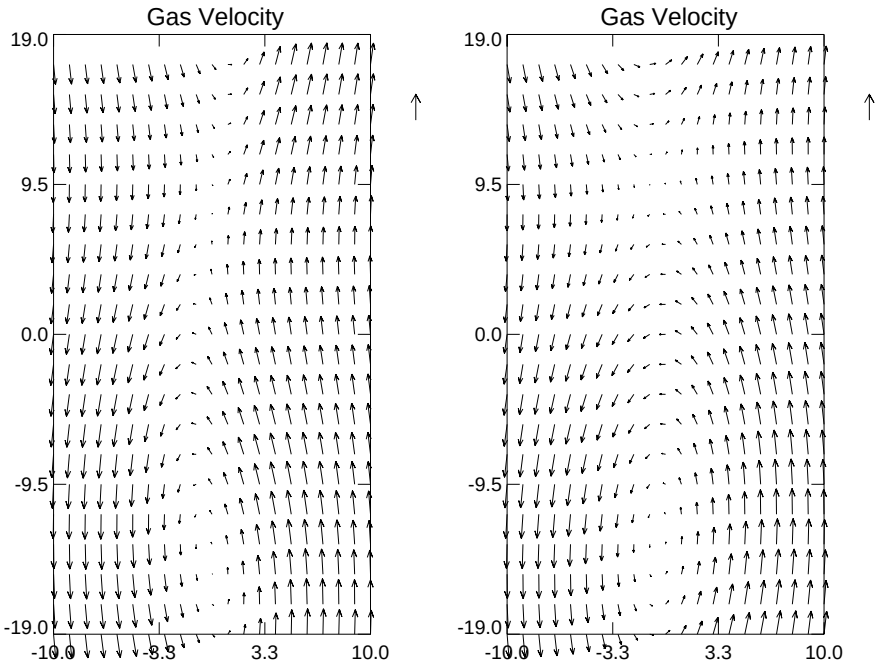

Fig. 7. Neutral gas velocity (indicated by arrows) after $t = 100t_A$ (left plot) and $t = 250t_A$ (right plot). As in the ionized fluid component the KH mode structure can easily be identified. The lengths of the exposed arrows indicate a flow velocity magnitude of 1.20 and 1.21 times the initial amplitude.

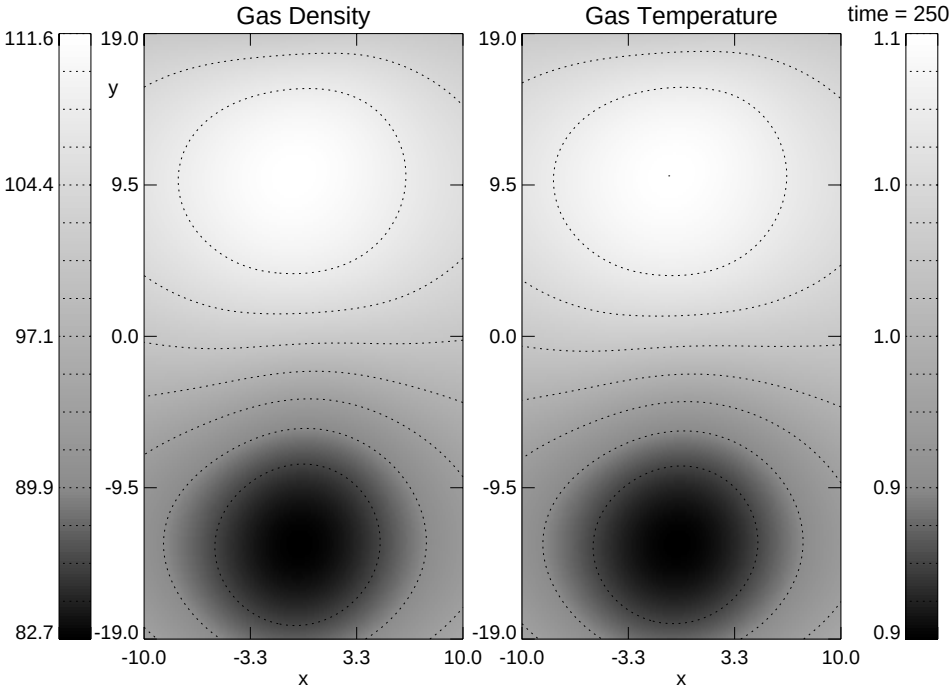

Fig. 8. Density and temperature of the neutral gas component after $t = 250t_A$. Regions of compression and depletion are located in the plane of the shear flow similar to the ones for the ionized component.

Also, the interaction of different vortices excited in neighbored resonant layers should be considered in order to get reliable quantitative results for the amplification factor of the magnetic field. Such an interaction is to be expected since there should be numerous KH resonant layers in the highly filamentary superwinds (cf. Reuter et al. 1992). The description of the whole scenario of magnetic field amplification and flux redistribution is beyond the scope of the present contribution. A self-consistent numerical 3D-analysis to elaborate on the discussed processes will be addressed in future work.

The KH instability discussed here can be regarded as a general and basic plasma process that occurs in complex, one- and multifluid shear flows. Our analysis of KH modes in partially ionized plasma régimes should also have applications to the dynamics of accretion disks in active galactic nuclei, X-ray binary systems, and in the disks around young stellar objects.

Appendix A

We consider streams of neutral and ionized gas components that flow in parallel directions on either side of the KH interface with

different bulk velocities and mass densities. In the unperturbed state the interface, say $y = 0$, is horizontal. Let be $\mathbf{v}^{eq} = v_{II}\mathbf{e}_z$, $\rho^{eq} = \rho_{II}$, $\mathbf{v}_n^{eq} = v_{nII}\mathbf{e}_z$, and $\rho_n^{eq} = \rho_{nII}$ for $y > 0$ and $\mathbf{v}^{eq} = v_I\mathbf{e}_z$, $\rho^{eq} = \rho_I$, $\mathbf{v}_n^{eq} = v_{nI}\mathbf{e}_z$, and $\rho_n^{eq} = \rho_{nI}$ for $y < 0$, where ρ and $\mathbf{v}$ denote the mass density and the bulk velocity. The index n is used to indicate the neutral gas quantities. We assume that in the basic state there is a uniform, horizontal magnetic field parallel to the flow (which is the least favorable situation for the KH instability to set in) $\mathbf{B}^{eq} = B\mathbf{e}_z$. Moreover, for the analytical calculations we assume incompressibility and that the convective term in the induction equations dominates the small resistive one, for mathematical convenience. The basic set of the linearized equations is given by

$$\nabla \cdot \mathbf{v}_1 = 0 \tag{A.1}$$

$$\nabla \cdot \mathbf{v}_{n1} = 0 \tag{A.2}$$

$$\left(\frac{\partial}{\partial t} + \mathbf{v}^{eq}\nabla\right)\rho_1 + \mathbf{v}_1\nabla\rho^{eq} = 0 \tag{A.3}$$

$$\left(\frac{\partial}{\partial t} + \mathbf{v}_n^{eq}\nabla\right)\rho_{n1} + \mathbf{v}_{n1}\nabla\rho_n^{eq} = 0 \tag{A.4}$$

$$\rho^{eq}\left(\frac{\partial}{\partial t} + \mathbf{v}^{eq}\cdot\nabla\right)\mathbf{v}_1 = -\nabla p_1 + \frac{1}{4\pi}(\nabla\times\mathbf{B}_1)\times\mathbf{B}^{eq} - \rho^{eq}\nu(\mathbf{v}_1 - \mathbf{v}_{n1}) \tag{A.5}$$

$$\rho_n^{eq}\left(\frac{\partial}{\partial t} + \mathbf{v}_n^{eq}\cdot\nabla\right)\mathbf{v}_{n1} = -\nabla p_{n1} + \rho^{eq}\nu(\mathbf{v}_1 - \mathbf{v}_{n1}) \tag{A.6}$$

$$\frac{\partial}{\partial t}\mathbf{B} = \nabla\times(\mathbf{v}_1\times\mathbf{B}^{eq} + \mathbf{v}^{eq}\times\mathbf{B}_1) \tag{A.7}$$

where p, B, and ν denote the thermal pressure, the magnetic field, and the effective plasma-neutral gas elastic collision frequency, respectively. The index 1 indicates the perturbed quantities. These are assumed to be of the form $\Phi = \hat{\Phi}(y)\exp(i(k_x x + k_z z - \omega t))$ with the complex frequency ω and the wave numbers of the modes k_x and k_z. With this form of perturbations we find six algebraic equations to be solved for the x- and y-components of the perturbed flows and the perturbed pressures. For the x-component of Eq. (A5), multiplied by $i\tilde{\omega}$ where $\tilde{\omega} = \omega - k_z v^{eq}$ is the Doppler shifted frequency, and the y-component of Eq. (A5) multiplied by $\tilde{\omega}$ we obtain

$$-i\frac{{B^{eq}}^2}{4\pi}k_x\frac{\partial}{\partial y}v_{y1} - \Big(\tilde{\omega}^2\rho^{eq} - \frac{{B^{eq}}^2}{4\pi}(k_x^2 + k_z^2) + i\tilde{\omega}\nu\rho^{eq}\Big)v_{x1} + i\tilde{\omega}\nu\rho^{eq}v_{nx1} + \tilde{\omega}k_x p_1 = 0 \tag{A.8}$$

$$-i\left(\tilde{\omega}^2\rho^{eq} - \frac{{B^{eq}}^2}{4\pi}k_z^2 + i\tilde{\omega}\nu\rho^{eq}\right)v_{y1} - i\frac{{B^{eq}}^2}{4\pi}\frac{\partial^2}{\partial y^2}v_{y1} + \frac{{B^{eq}}^2}{4\pi}k_x\frac{\partial}{\partial y}v_{x1} - \tilde{\omega}\nu\rho^{eq}v_{ny1} + \tilde{\omega}\frac{\partial}{\partial y}p_1 = 0 \tag{A.9}$$

where we made use of Eq. (A7) and here and in the following we omitted the hat indicating the amplitudes of the perturbed quantities. With the help of Eqs. (A1) and (A2) we find for the z-component of Eq. (A5) multiplied by $-i\tilde{\omega}k_z$

$$\tilde{\omega}\rho^{eq}(\nu - i\tilde{\omega})\frac{\partial}{\partial y}v_{y1} + k_x\tilde{\omega}\rho^{eq}(\tilde{\omega} + i\nu)v_{x1} - \tilde{\omega}\nu\rho^{eq}\frac{\partial}{\partial y}v_{ny1} - i\tilde{\omega}\nu k_x\rho^{eq}v_{nx1} + \tilde{\omega}k_z^2 p_1 = 0. \tag{A.10}$$

The Cartesian components of the neutral gas momentum balance equation (A6) give accordingly

$$-(\tilde{\omega}_n^2\rho_n^{eq} + i\tilde{\omega}_n\nu\rho^{eq})v_{nx1} + i\tilde{\omega}_n\nu\rho^{eq}v_{x1} + \tilde{\omega}_n k_x p_{n1} = 0 \tag{A.11}$$

$$(-i\tilde{\omega}_n^2\rho_n^{eq} + \tilde{\omega}_n\nu\rho^{eq})v_{ny1} - \tilde{\omega}_n\nu\rho^{eq}v_{y1} + \tilde{\omega}_n\frac{\partial}{\partial y}p_{n1} = 0 \tag{A.12}$$

$$(-i\tilde{\omega}_n^2\rho_n^{eq} + \tilde{\omega}_n\nu\rho^{eq})\frac{\partial}{\partial y}v_{ny1} + (k_x\tilde{\omega}_n^2\rho_n^{eq} + ik_x\tilde{\omega}_n\nu\rho^{eq})v_{nx1} - \tilde{\omega}_n\nu\rho^{eq}\frac{\partial}{\partial y}v_{y1} - i\tilde{\omega}_n\nu\rho^{eq}k_x v_{x1} + \tilde{\omega}_n k_z^2 p_{n1} = 0 \tag{A.13}$$

where $\tilde{\omega}_n$ denotes the Doppler shifted frequency $\tilde{\omega}_n = \omega - k_z v_n^{eq}$. We concentrate on surface waves that decay exponentially with increasing distance from the boundary layer $v_{y1} = v_{y1}(0)exp(\mp k_y y)$ and $v_{ny1} = v_{ny1}(0)exp(\mp k_y y)$ where the minus signs holds for $y > 0$ and the plus sign for $y < 0$. We assume that the boundary layer is not a discontinuity but that the physical quantities vary continuously across the small finite width of the interface. It is reasonable to assume that the tangential velocity perturbations, the pressure perturbations as well as $\partial v_{y1}/\partial y$ and $\partial v_{ny1}/\partial y$ are odd functions of y. Denoting the 'jumps' by brackets we find

$$[v_{y1}] = 0 \;;\; \left[\frac{\partial}{\partial y}v_{y1}\right] = -2k_y v_{y1}(0)$$
$$[\tilde{\omega}^2\rho^{eq}v_{x1}] = \overline{\tilde{\omega}^2\rho^{eq}}[v_{x1}]$$
$$\left[\tilde{\omega}^2\rho^{eq}\frac{\partial}{\partial y}v_{y1}\right] = -2k_y\overline{\tilde{\omega}^2\rho^{eq}}v_{y1}(0) \tag{A.14}$$

where the bar denotes the mean values across the interface $\overline{\Phi} = 0.5(\Phi_1 + \Phi_2)$, and

$$\int_I^{II}\tilde{\omega}\frac{\partial}{\partial y}p_1 dy = [\tilde{\omega}p_1] - \int_I^{II}\frac{\partial}{\partial y}\tilde{\omega}p_1 dy = [\tilde{\omega}p_1]. \tag{A.15}$$

Eqs. (A14) and (A15) hold accordingly for the neutral gas quantities. After integrating Eqs. (A9) and (A12) over y non-trivial solutions for the homogeneous equations for $[v_{x1}]$, $iv_{y1}(0)$, $[\tilde{\omega}p_1]$, $[v_{nx1}]$, $iv_{ny1}(0)$, and $[\tilde{\omega}_n p_{n1}]$ require the coefficient determinate to be zero, i.e.

$$16\pi^2 i(\nu\overline{\tilde{\omega}_n\rho^{eq}} - \overline{\tilde{\omega}_n^2\rho_n^{eq}})^2\overline{\tilde{\omega}^2\rho^{eq}}^2 + 8\pi[{B^{eq}}^2k_z^2(-i\nu^2\overline{\tilde{\omega}_n\rho^{eq}}^2 + i\overline{\tilde{\omega}_n^2\rho_n^{eq}}^2 - 2\nu\overline{\tilde{\omega}_n\rho^{eq}}\,\overline{\tilde{\omega}_n^2\rho_n^{eq}}) + 4\pi\nu\overline{\tilde{\omega}\rho^{eq}}(\overline{\tilde{\omega}_n^2\rho_n^{eq}}^2 + i\nu\overline{\tilde{\omega}_n\rho^{eq}}\,\overline{\tilde{\omega}_n^2\rho_n^{eq}})]\overline{\tilde{\omega}^2\rho^{eq}}$$

$$+B^{eq^4}k_z^4(-i\overline{\tilde{\omega}_n^2\rho_n^{eq}}^2+2\nu\overline{\tilde{\omega}_n\rho^{eq}}\overline{\tilde{\omega}_n^2\rho_n^{eq}}+i\nu^2\overline{\tilde{\omega}_n\rho^{eq}}^2)$$
$$-8\pi B^{eq^2}k_z^2\nu\overline{\tilde{\omega}\rho^{eq}}\overline{\tilde{\omega}_n^2\rho_n^{eq}}(i\nu\overline{\tilde{\omega}_n\rho^{eq}}+\overline{\tilde{\omega}_n^2\rho_n^{eq}})$$
$$+16\pi^2 i\nu^2\overline{\tilde{\omega}\rho^{eq}}^2\overline{\tilde{\omega}_n^2\rho_n^{eq}}^2=0. \quad \text{(A.16)}$$

Eq. (A16) represent the generalized dispersion relation for the KH modes in partially ionized plasmas. For $\nu = 0$ is reduces to the well-known dispersion relation for fully ionized plasmas (see e.g. Woods 1987)

$$\left(\frac{B^{eq^2}}{4\pi}k_z^2-\overline{\tilde{\omega}^2\rho^{eq}}\right)^2=0. \quad \text{(A.17)}$$

Acknowledgements. We would like to thank the referee for his helpful comments. This work was supported by the Deutsche Forschungsgemeinschaft through the grant LE 1039/2-1, 3-1 and the NATO Scientific Collaboration Grants program. GTB also gratefully acknowledges support by the AvH foundation through a Fedor Lynen fellowship, in the course of which substantial parts of this contribution were developed. PPK acknowledges support from the Natural Science and Engineering Research Council of Canada, and of a Killam Fellowship.

References

Bhatia P.K., Steiner J.M., 1974, Aust. J. Phys. 27, 53
Biermann L., Schlüter A., 1951, Phys. Rev. 82, 863
Birk G.T., Otto A., 1996, J. Comp. Phys. 125, 513
Birk G.T., Wiechen H., Otto A., 1999, ApJ 518, 177
Clarke D.A., 1993, In: Röser H.J., Meisenheimer K. (eds.) Jets in Extragalactic Radio Sources. Springer, Berlin, p. 243
Dahlem M., Petr M.G., Lehnert M.D., Heckman T.M., Ehle M.D., 1997, A&A 320, 731
Duric N., Seaquist E.R., Crane P.C., Bignell R.C., Davis L.E., 1983, ApJ 273, L11
Ershkovich A.I., Mendis D.A., 1983, ApJ 269, 743
Ershkovich A.I., Mendis D.A., 1986, ApJ 302, 849
Ershkovich A.I., Prialnik D., Eviatar A., 1986a, J. Geophys. Res. 91, 8782
Ershkovich A.I., Flammer K.R., Mendis D.A., 1986b, ApJ 311, 1031
Frank A., Jones T.W., Ryu D., Gaalaas J.B., 1996, ApJ 460, 777
Heckman T., 1998, ASP Conf. Ser. 148, 126
Heckman T., Lehnert M.D., Armus L., 1993, In: Shull J.M., Thronson Jr. H.A. (eds.) The Environment and Evolution of Galaxies. Kluwer, Dordrecht, p. 455
Hummel E., Lesch H., Wielebinski R., Schlickeiser R., 1988, A&A 197, L29
Jones T.W., Ryu D., Frank A., 1999, In: Miyama S., Tomisaka K., Hanawa T. (eds.) Numerical Astrophysics. Kluwer, Dordrecht, p. 95
Kronberg P.P., 1994, Rep. Prog. Phys. 57, 325
Kronberg P.P., Lesch H., Hopp U., 1999, ApJ 511, 56
Lehnert M.P., Heckman T.M., 1996, ApJ 462, 651
Lesch H., Chiba M., 1995, A&A 297, 305
MacLow M.M., Ferrara A., 1999, ApJ 513, 142
Mateo M.L., 1998, ARA&A 36, 435
McKeith C.D., Greve A., Downes D., Prada F., 1995, A&A 293, 703
Miniati F., Ryu D., Ferrara A., Jones T.W., 1999, ApJ 510, 726
Nath B.B., Chiba M., 1995, ApJ 454, 604
Padmanabhan T., 1993, Structure formation in the universe. Cambridge University Press, Cambridge
Renzini A., 1997, ApJ 488, 35
Reuter H.-P., Klein U., Lesch H., Wielebinski R., Kronberg P.P., 1992, A&A 256, 10
Rieke G.H., Lebofsky M.J., Thompson R.I., Low F.J., Tokunaga A.T. 1980, ApJ 238, 24
Shopbell P.L., Bland-Hawthorn J., 1998, ApJ 493, 129
Tegmark M., Silk J., Rees M.J., et al., 1997, ApJ 474, 1
Trentham N., 1994, Nat 372, 157
Weiß A., Walter F., Neininger N., Klein U., 1999, A&A 345, L23
Woods L.C., 1987, Principles of Magnetohydrodynamics. Claredon Press, Oxford, p. 163